A Neutron Diffraction Investigation of the Defect Rutile Structure of Tin–Antimony Oxide

By **Frank J. Berry** and **Colin Greaves**, Department of Chemistry, University of Birmingham, P.O. Box 363, Birmingham B15 2TT

The defect structure of tin–antimony oxide has been investigated by profile refinement of powder neutron diffraction data. The structure, based on the occupation by antimony(III) of interstitial positions within the tin(IV) oxide rutile-type lattice, is described and the model used to rationalise some of the properties of the mixed oxide.

THE structural properties of tin–antimony oxides have been the subject of confusion for many years with materials prepared by apparently similar methods having been given different descriptions.[1] Even recent studies by electron microscopy [2] and *X*-ray diffraction [3,4] are, as has been acknowledged,[3] not unequivocal in their interpretation. Poor crystallinity [3,4] precludes accurate structural investigation by *X*-ray diffraction and the absence of long-range defect ordering limits investigation by electron microscopy. The lack of clarity concerning the fundamental structural details inhibits complete rationalisation of other recent studies of surface [5,6] and electrical properties.[7] These physical characteristics are technologically important since tin–antimony oxides have been developed as catalysts for the selective oxidation and ammoxidation of hydrocarbons [1] and are potential electrode materials for the photoassisted electrolysis of water.[8] The absence of an accurate structural description has prevented elucidation of the relationship between these properties and fundamental structural features.

The use of neutron diffraction is, in principle, a powerful means by which the structure of tin–antimony oxides may be investigated since it enables the acquisition of reliable structural data from powder samples using profile refinement techniques. We have therefore conducted a powder neutron diffraction study of tin–antimony oxide from the monophasic rutile-type region of the phase diagram recently established by a comprehensive *X*-ray investigation.[3] We have also attempted to rationalise other properties of the material in terms of the structural model we propose.

EXPERIMENTAL

Tin–antimony oxide with a nominal antimony : tin ratio of 1 : 10 was prepared by the simultaneous addition of anhydrous tin(IV) chloride and antimony(V) chloride to ammonium hydroxide solution. The alkalinity of the mixture was maintained by addition of NH_4OH. The white precipitate was removed by filtration, washed, dried at 120 °C, ground, and calcinated in air for 6 h at 600 °C. The mean crystallite size, estimated from *X*-ray diffraction line broadening, of *ca.* 7 nm was considered too small for accurate structural analysis by neutron diffraction. Heating for 72 h at 800 °C induced crystal growth to *ca.* 14 nm. Despite the inherently reduced resolution of neutron diffraction relative to *X*-ray diffraction, such materials would still be expected to give broadened neutron diffraction peaks. However, given the significant loss of antimony which occurs at elevated temperature [3,5] the sample was not subjected to further thermal treatment.

Chemical analysis for Sn and Sb of the product by atomic absorption spectroscopy showed an antimony content, relative to that of tin, of $10.6 \pm 0.3\%$ which corresponds to an overall stoicheiometry for the material of $MO_{1.99 \pm 0.06}$ (M = Sn, Sb).

Neutron diffraction data were collected at ambient temperature on the PANDA diffractometer at A.E.R.E., Harwell using neutrons of wavelength 1.5397 Å from the 115 planes of a germanium monochromator with a 90° take-off angle. Scattering lengths of $(0.61, 0.56, 0.58) \times 10^{-12}$ cm respectively were used for tin, antimony, and oxygen. Absorption corrections were not necessary. Structural parameters were refined by standard profile techniques [9] involving a least-squares procedure to minimise a profile index R_{pw}, based on the appropriately weighted observed counts at each point of the profile and the counts calculated for the particular model. An unweighted residual R_p was calculated after each refinement cycle. The observed and calculated peak intensities estimated from the peak half-width parameters enabled the calculation of a more conventional R_I index.

^{119}Sn and ^{121}Sb Mössbauer data were recorded with a conventional constant-acceleration spectrometer with source and absorber at identical temperatures. ^{119}Sn spectra were recorded with a $Ca^{119m}SnO_3$ source (m denotes metastable isotope) at 77 K and ^{121}Sb spectra were obtained with a $Ba^{121m}SnO_3$ source at 4 K. The drive velocity was calibrated with a ^{57}Co/Rh source and iron foil. The spectra were computer-fitted.

RESULTS AND DISCUSSION

The antimony content of $10.6 \pm 0.3\%$ in a material of composition $MO_{1.99 \pm 0.06}$ is insufficiently precise to differentiate between structural models based on Sb^{III} or Sb^{V} in a tin oxide matrix for which the ^{119}Sn Mössbauer spectrum shows the presence of only Sn^{IV}.

The neutron diffraction profile was consistent with a single rutile-type phase; the peak half-widths did not correspond with the instrumental resolution but were consistent with broadening as expected for a mean crystallite size of *ca.* 14 nm. Refinement was based on a tetragonal unit cell, space group $P4_2/mnm$, $Z = 2$.

Initially a statistical distribution of 10.6% Sb on tin sites was assumed and the total metal occupation parameter refined relative to oxygen being 2.0. Thermal

parameters were assumed isotropic. The refined occupation number, 0.919(12), clearly indicated a metal deficit. Refinement indexes $R_{pw} = 0.122$, $R_p = 0.139$, and $R_I = 0.060$ were obtained; the R_{pw} value expected for discrepancies from counting statistics was 0.080. Although the indexes were satisfactory the model was considered unacceptable on grounds of charge balance. The refinement implied that the antimony content of 10.6% would be associated with the unsatisfactory mean antimony oxidation state of 7.7(6). An alternative interpretation based on Sb^V would demand an Sb : Sn ratio of *ca.* 50 : 50 observed, calculated, and difference profiles are shown in Figure 1.

The antimony occupation parameter [equivalent to Sb/Sn = 11.8(1.2)%] is in agreement with the chemical analysis. The refined atomic co-ordinates indicate that the antimony atoms are displaced by 1.2 Å from the octahedral interstice (0, 0.5, 0.5) to a position (−0.055, 0.283, 0.326) which is 1.0 Å from an oxygen site (−0.1954, 0.1954, 0.5) and 1.7 Å from the tin site at the origin. The refined antimony position does not allow the occupation of either the tin or the oxygen site. In this respect

TABLE 1

Structural parameters for tin–antimony oxide, with estimated standard deviations in parentheses

Atom	Position	*x*	*y*	*z*	*B*/Å²	Relative occupation per cell	Absolute occupation for proposed model
Sn	2a	0	0	0	0.29(8)	0.918(7)	0.871(7)
Sb	16k	−0.055(13)	0.283(18)	0.326(18)	0.29(8)	0.109(10)	0.103(10)
O	4f	0.304 6(3)	*x*	0	0.68(5)	2.0	1.897(10)

Cell parameters $a = b = 4.737\ 3(5)$, $c = 3.181\ 6(5)$ Å

Bond distances (Å)

Sb–O(1)	2.00(12)	Sb–O(4)	2.79(12)
Sb–O(2)	2.74(12)	Sb–O(5)	2.74(12)
Sb–O(3)	2.51(12)	Sb–O(6)	2.62(12)

Bond angles (°)

O(2)–Sb–O(3)	66.9(2.3)	O(1)–Sb–O(2)	73.6(2.0)
O(3)–Sb–O(4)	66.0(3.2)	O(1)–Sb–O(3)	98.5(1.9)
O(4)–Sb–O(5)	63.1(3.0)	O(1)–Sb–O(4)	72.3(3.0)
O(5)–Sb–O(6)	65.5(3.0)	O(1)–Sb–O(5)	82.8(1.0)
O(6)–Sb–O(2)	100.5(1.2)	O(1)–Sb–O(6)	76.6(3.0)

which is also totally unrealistic in view of the chemical analysis. Moreover, a model involving substitutional Sb^V and metal vacancies would be inconsistent with n-type semiconductor behaviour.

An alternative model may be envisaged involving interstitial antimony within the chains of vacant octahedral sites of the rutile-type structure. Such a model requires charge balance by vacant sites on the tin sublattice. Since the electrical properties of tin–antimony oxide imply the presence of Sb^{III} rather than Sb^V, the incorporation of 10.6% Sb may be associated with the creation of *ca.* 7% unoccupied tin sites which is consistent with the initial refinement.

Further refinements using this model produced improved profile residuals. The antimony isotropic temperature factor was highly correlated with the antimony occupation parameter and in the final refinement was constrained equal to that of tin. An additional constraint was applied to maintain charge balance in accordance with the presence of only Sb^{III}. The residuals $R_{pw} = 0.117$, $R_p = 0.132$, $R_I = 0.055$ were obtained after refinement of the scale factor, zero-point error, three half-width parameters, two cell parameters, four positional parameters, two isotropic temperature factors, and one occupation parameter. Removal of the charge balance constraint was deemed unwarranted by the very slight improvement in the resultant residuals. Refined structural data are given in Table 1. The it is significant that the anomalously low densities of many B-metal materials have been explained [10] by lone-pair occupation of anionic sites about 1 Å away from the B-metal atom. Hence, the close proximity of an anionic vacancy to an Sb^{III} species in the structure proposed here may be associated with the accommodation of a stereochemically active lone pair. The vacant proximal cationic site is consistent with charge balance in a system containing antimony(III)–oxygen vacancy pairs with a net charge of 5+. The absolute site occupancies appropriate to this model are included in Table 1.

The above model may also be visualised in terms of the substitution of Sb^{III} for Sn^{IV} in tin(IV) oxide, the introduction of oxygen vacancies to accommodate the stereochemical requirements of the lone pairs on Sb^{III}, and of cationic vacancies to maintain charge balance. The migration of Sb^{III} to the lower symmetry sites close to the anionic vacancies would in itself create additional cationic vacancies.

The above refinement based on an average unit cell implies a co-ordination about tin which is essentially the same as that in tin(IV) oxide. However, on a local atomic level the presence of oxygen vacancies might reasonably be expected to give rise to modified co-ordination for many of the atoms.

The low-symmetry antimony site may be described as a highly distorted pentagonal prism with O(1) at the apex. The equatorial angles are equal except for the

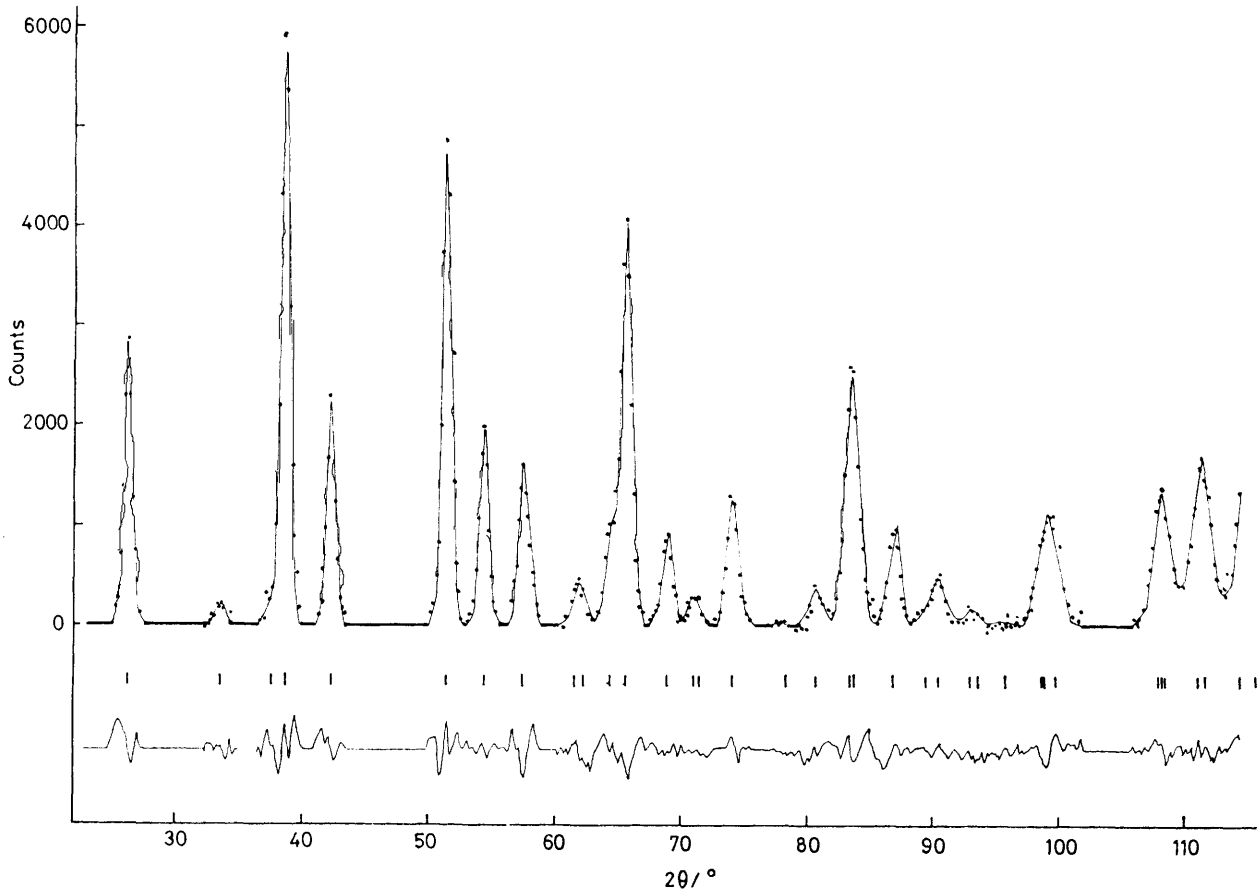

FIGURE 1 Experimental (· · · ·) and calculated (——) neutron diffraction profiles. The positions of the reflections and the difference profile (bottom) are also indicated

larger O(6)–Sb–O(2) angle which reflects the vacant metal site midway between O(6) and O(2). The lone pair occupies the seventh position of a pentagonal-bipyramidal array. The antimony co-ordination is shown in Figure 2 projected along [010]. Finally, it is relevant to note that ' antimony–metal vacancy–oxygen vacancy ' clusters may produce relaxation of neighbouring atoms which cannot be totally represented in the above description.

The refined cell parameters indicate a slight contraction along the c axis relative to tin(IV) oxide [11] ($a = b = 4.7373$, $c = 3.1864$ Å) and presumably reflect the reduction by the cationic vacancies of the metal–metal electrostatic interactions in a structure consisting of chains of edge-sharing octahedra parallel to the c axis.

The structure described above is unusual in that both anion and cation sub-lattices are imperfect, and also differs markedly from other recent descriptions [7,12] which have sought to explain the electrical behaviour of tin–antimony oxides. In order to compare the validity of the different structural descriptions, it is necessary to examine their compatibility with the reported electrical properties. The n-type conductivity of pure tin(IV) oxide, which has been attributed [13] to oxygen vacancy donor levels, is known to be increased by reduction [12–14] or doping with antimony.[7,12,15–17] At low conduction electron concentrations ($<10^{18}$ cm^{-3}) reduced and antimony–doped tin(IV) oxides have primary donor levels approximately 30 meV * below the conduction

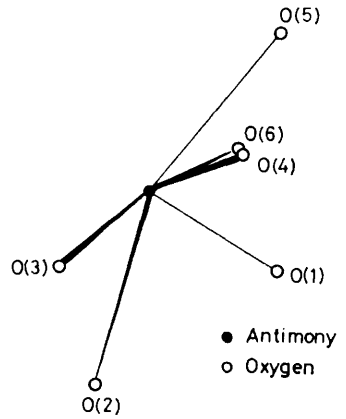

FIGURE 2 Co-ordination of antimony projected along [010]

band which have been assigned to either oxygen vacancies [18] or dopant antimony.[19] When the conduction electron concentrations exceed 10^{19} cm^{-3} the donor band

* Throughout this paper: 1 eV = 1.602 19 × 10^{-19} J.

merges with the main conduction band and gives a degenerate semiconductor [12,14] in which the conduction electron concentration and resistivity are independent of temperature. Such a band structure is obtained at antimony concentrations as low as 300 p.p.m.,[12] and implies complete delocalisation of the donor electrons. According to our structural model, this is equivalent to the incorporation of the Sb^{III} lone-pair orbitals into the bonding scheme resulting in partial occupation of the conduction band.

The previous explanations of the electrical behaviour of tin–antimony oxides [7,12] assumed donor centres in which an electron, associated with an Sb^{5+} ion to maintain charge balance, can be promoted into the conduction band. Since this model implies the formation of Sb^{4+}, which has little chemical significance, our description appears preferable from a chemical viewpoint. It also offers a better rationalisation of the similarity in the band structures of reduced and antimony-doped materials (see above), since the Sb^{III} lone pairs directed into oxygen vacancies may be envisaged as donor levels which would be expected to correspond quite closely to un-ionised oxygen vacancies. In this respect, it is interesting that e.s.r. signals from antimony-doped tin(IV) oxide have been interpreted [20] in terms of singly ionised oxygen vacancies.

Although totally incompatible with our neutron diffraction study, the model involving (Sb^{5+}–e^-) donors can account [7] for ^{121}Sb Mössbauer data which have implied Sb^V as the major antimony species. In view of this, we have investigated our material by Mössbauer spectroscopy. The ^{119}Sn Mössbauer chemical isomer shift δ (Table 2) is characteristic of a Sn^{IV} species in an oxygen environment.[21] The quadrupole splitting Δ is slightly larger than that of tin(IV) hydroxide gel dehydrated [21] at 800 °C (δ 0.00 mm s^{-1}, Δ 0.56 mm s^{-1}) and reflects the increased electric-field gradient at the tin nuclei as a result of antimony incorporation within the tin(IV) oxide lattice. The two-peaked ^{121}Sb Mössbauer spectrum is, on first inspection, indicative of the presence of both Sb^V and Sb^{III} in the ratio *ca.* 6 : 1. Since $\Delta R/R$ is negative for the ^{121}Sb transition,[22] the Sb^{III} chemical isomer shifts are more negative than those of Sb^V. The species appearing as Sb^V has a more negative chemical isomer shift than is normally expected for Sb^V in rutile-type structures [23,24] which is indicative of a higher electron density at antimony and consistent with the delocalisation of the lone-pair electrons on the interstitial Sb^{III} into conduction bands. Similar effects, albeit to a lesser extent, have been observed in the Mössbauer spectra of other antimony- [25] and tin-containing [26–29] solids. The linewidth of the Sb^{III} resonance peak, although not amenable to fitting according to a quadrupole-split model, is broader than that observed in crystalline antimony compounds, and the chemical isomer shift is more negative than for Sb_2O_3,[30,31] implying a higher *s*-electron density at the Sb^{III} nuclei. The spectrum is therefore consistent with the occupation by Sb^{III}, with predominantly *p*-character stereochemically active lone pairs, of more asymmetric sites than those adopted in Sb_2O_3. Given the presence of only Sb^V in a material of similar composition heated at lower temperature [32] the presence of Sb^{III} in the material investigated here may be associated with thermally induced surface enrichment in antimony [5,6] and the more favourable accommodation of Sb^{III} in asymmetric surface sites. Indeed, *X*-ray photoelectron spectroscopy studies [5,6,33] have indicated the presence of only Sb^{III} at the surface of antimony-containing oxides and reflect the more favourable accommodation of these species with stereochemically active lone pairs at surface sites. Although the neutron diffraction data alone do not suggest such migration, the uncertainty associated with the refined antimony occupation parameter is compatible with antimony depletion to the extent implied by the Mössbauer peak-area ratio.

TABLE 2

Mössbauer parameters of tin–antimony oxides

^{119}Sn		^{121}Sb				
		Sb^V		Sb^{III}		
δ [a]/mm s^{-1}	Δ/mm s^{-1}	δ [b]/mm s^{-1}	Γ/mm s^{-1}	δ [b]/mm s^{-1}	Γ/mm s^{-1}	Area ratio Sb^{III}/Sb^V
0.03 ± 0.03	0.64 ± 0.03	8.41 ± 0.1	3.60	−5.38 ± 0.1	5.40	0.16

[a] δ Relative to SnO_2. [b] δ Relative to InSb.

The proposed structure is unusual in that it is based on rutile in which both anion and cation sub-lattices are incomplete. However, the inherent instability of such a structure appears to be offset by the reduction in *c* due to reduced electrostatic repulsions and the interaction of the antimony lone-pair electrons with the tin(IV) oxide band structure. A related stabilisation mechanism involving lone-pair participation in bonding has been proposed for the defect pyrochlore structure of $Pb_2Ru_2O_{7-x}$ and related phases.[34] Notwithstanding such stabilisation, the tin–antimony oxide dissociates at temperatures exceeding *ca.* 900 °C to an equilibrated solid solution of 4% Sb in tin(IV) oxide and an Sb_2O_4 phase which is volatilised.[3]

We acknowledge the provision by the S.R.C. of neutron diffraction facilities at A.E.R.E., Harwell and we are grateful to Inco Europe Ltd., for chemical analysis.

[1/433 *Received*, 17*th March*, 1981]

REFERENCES

[1] D. J. Hucknall, 'Selective Oxidation of Hydrocarbons,' Academic Press, London, 1974, p. 42.
[2] D. Pyke, R. Reid, and R. J. D. Tilley, *J. Solid State Chem.*, 1978, **25**, 231.

[3] D. Pyke, R. Reid, and R. J. D. Tilley, *J. Chem. Soc., Faraday Trans. 1*, 1980, 1174.
[4] J. L. Portefaix, P. Bussiere, M. Forissier, F. Figueras, J. M. Friedt, J. P. Sanchez, and F. Theobald, *J. Chem. Soc., Faraday Trans. 1*, 1980, 1652.
[5] Y. M. Cross and D. Pyke, *J. Catal.*, 1979, **58**, 61.
[6] Y. Boudeville, F. Figueras, M. Forissier, J. L. Portefaix, and J. C. Vedrine, *J. Catal.*, 1979, **58**, 52.
[7] J. M. Herrmann, J. L. Portefaix, M. Forissier, F. Figueras, and P. Pichat, *J. Chem. Soc., Faraday Trans. 1*, 1979, 1346.
[8] M. S. Wrighton, D. L. Morse, A. B. Ellis, D. S. Ginley, and M. B. Abrahamson, *J. Am. Chem. Soc.*, 1976, **98**, 44.
[9] H. M. Rietveld, *J. Appl. Crystallogr.*, 1969, **2**, 65.
[10] S. Andersson and A. Astrom in ' Solid State Chemistry,' eds. R. S. Roth and J. S. Schnieider, National Bureau of Standards, spec. publ. 364, Washington, 1972, p. 3.
[11] H. Schrocke, *Neues Jahrb. Mineral. Monatsh.*, 1959, 97.
[12] J. A. Marley and R. C. Dockerty, *Phys. Rev., Sect. A*, 1965, **140**, 304.
[13] Z. M. Jarzebski and J. P. Marton, *J. Electrochem. Soc.*, 1976, **123**, 299C.
[14] M. Nagasawa and S. Shionoya, *Jpn. J. Appl. Phys.*, 1971, **10**, 472.
[15] E. J. Leja, *Acta Phys., Pol. A*, 1970, **38**, 165.
[16] G. W. Godin, C. C. McCain, and E. A. Porter, Proceedings of the 4th International Congress on Catalysis, Moscow, 1968, ed. D. A. Kuzanaski, Akademiai Kiado, Budapest, 1971.
[17] K. Wakabayashi, Y. Kamiya, and N. Ohta, *Bull. Chem. Soc. Jpn.*, 1968, **41**, 2776.
[18] S. Samson and C. G. Fonstad, *J. Appl. Phys.*, 1973, **44**, 4618.
[19] C. G. Fonstad and R. H. Rediker, *J. Appl. Phys.*, 1971, **42**, 2911.
[20] F. J. Berry and J. C. McAteer, *Inorg. Chim. Acta*, 1981, **50**, 85.
[21] F. J. Berry and A. G. Maddock, *Radiochim. Acta*, 1977, **24**, 32.
[22] N. N. Greenwood and T. C. Gibb, ' Mossbauer Spectroscopy,' Chapman and Hall, London, 1971, p. 449.
[23] J. B. Wooten, G. C. Long, and L. H. Bowen, *J. Inorg. Nucl. Chem.*, 1974, **36**, 2177.
[24] J. D. Donaldson, A. Kjekshus, D. G. Nicholson, and T. Rakke, *Acta Chem. Scand., Ser. A*, 1975, **29**, 803.
[25] J. D. Donaldson, D. R. Laughlin, and M. J. K. Thomas, *Radiochem. Radioanal. Lett.*, 1977, **28**, 91.
[26] J. Barrett, S. R. Bird, J. D. Donaldson, and J. Silver, *J. Chem. Soc. A*, 1971, 3105.
[27] J. D. Donaldson, D. Laughlin, S. D. Ross, and J. Silver, *J. Chem. Soc., Dalton Trans.*, 1973, 1985.
[28] J. D. Donaldson and J. Silver, *Inorg. Nucl. Chem. Lett.*, 1974, **10**, 537.
[29] J. D. Donaldson, J. Silver, S. Hadjiminolis, and S. D. Ross, *J. Chem. Soc., Dalton Trans.*, 1975, 1500.
[30] G. G. Long, J. G. Stevens, and L. H. Bowen, *Inorg. Nucl. Chem. Lett.*, 1969, **5**, 799.
[31] D. J. Stewart, O. Knop, C. Ayasse, and F. W. D. Woodhams, *Can. J. Chem.*, 1972, **50**, 690.
[32] F. J. Berry, P. E. Holbourn, and F. W. D. Woodhams, *J. Chem. Soc., Dalton Trans.*, 1980, 2241.
[33] A. F. Orchard and G. Thornton, *J. Chem. Soc., Dalton Trans.*, 1977, 1238.
[34] J. M. Longo, P. M. Raccah, and J. B. Goodenough, *Mater. Res. Bull.*, 1969, **4**, 191.